Stability of HEB receivers at THz frequencies

Therese Berg, Sergey Cherednichenko, Vladimir Drakinskiy, Pourya Khosropanah, Harald F. Merkel, et al.

Therese Berg, Sergey Cherednichenko, Vladimir Drakinskiy, Pourya Khosropanah, Harald F. Merkel, Erik L. Kollberg, Jacob W. Kooi, "Stability of HEB receivers at THz frequencies," Proc. SPIE 5498, Millimeter and Submillimeter Detectors for Astronomy II, (8 October 2004); doi: 10.1117/12.553162

Event: SPIE Astronomical Telescopes + Instrumentation, 2004, Glasgow, United Kingdom

Stability of HEB Receivers at THz Frequencies

T. Berg , S. Cherednichenko [1], V. Drakinskiy , P.Khosropanah , H. Merkel , E. Kollberg

Department of Microtechnology and Nanoscience, Chalmers University of Technology, Gothenburg, Sweden.

J.W. Kooi

California Institute of Technology, Pasadena, CA, USA

ABSRACT

Stability of a hot-electron bolometer (HEB) heterodyne receiver was investigated at frequencies from 0.6THz to 1.9THz. The Allan variance was measured as a function of the integration time and the Allan time was obtained for HEB mixers of different size, as well as with different types of the local oscillator: FIR laser, multiplier chain, and BWO. We have found that due to stronger dependence of the mixer gain and noise vs mixer bias voltage and current the Allan time is shorter for smaller mixers. At 1.6THz the Allan time is 3 sec for 4x0.4μm^2 bolometer, and 0.15-0.2 sec for 1x0.15μm^2 bolometer. Obtained stability appears to be the same for the FIR laser and the multiplier chain. The Allan time for smaller bolometers increases to 0.4-0.5sec at 0.6-0.7THz LO frequencies. The influence of the IF chain on the obtained results is also analyzed.

Keywords: HEB, mixer, receiver, heterodyne, THz, stability, NbN, superconductivity.

Introduction

Due to the atmosphere's low transmission at terahertz frequencies, the subMM and THz receivers used for radio astronomical observations are usually placed on high and dry places or sent out in space [Herschel, SOFIA, APEX, ASTRO]. To use the observation instruments on these very remote places is expensive. It is therefore important that the receivers are optimized in all aspects: noise temperature, local oscillator power, IF band, and stability.

Radio astronomical receivers generally detect very weak signals deeply embedded in noise. To extract the signal of interest, synchronous detection is used, i.e. the receiver is switched between on and off signal (e.g. by moving the beam on and off source) . However, since it takes a certain time to make this switch, high chopping frequency will interrupt the integration time with many black-out periods. Low chopping frequency prolongs observation time. However, longer integration time might be limited by the stability of the receiver.

According to the radiometer equation, for the case of white noise the square of the variance of the signal fluctuations reduces as $1/\tau$:

$$\sigma^2 = \frac{\langle x(t) \rangle^2}{B\tau}$$

---

[1] serguei.cherednichenko@mc2.chalmers.se

Millimeter and Submillimeter Detectors for Astronomy II, edited by
Jonas Zmuidzinas, Wayne S. Holland, Stafford Withington, Proceedings of
SPIE Vol. 5498 (SPIE, Bellingham, WA, 2004) · 0277-786X/04/$15 · doi: 10.1117/12.553162

where σ is the standard deviation of the signal fluctuations, $<x(t)>$ is the signal mean, B is the bandwidth and τ is the integration time.

Signal drift (modulation), and 1/f-noise in a real astronomical heterodyne receiver deviate σ^2 from $1/\tau$ dependence. For time periods longer than the time constants of the drift and 1/f noise the receiver noise is not uncorrelated anymore. In this case, integration for longer periods does not result in a better signal-to-noise ratio. A method to determine the optimum integration time for a system is to measure so called Allan variance [1] as a function of integration time.

Superconducting SIS receivers , as well as Schottky diode receivers, have been used for radio astronomical observations for long time already. A number of papers, describing their stability issues have been published [2]. 1THz threshold in heterodyne radio astronomy was triggered by development of superconducting hot- electron bolometer (HEB) mixers [3]. The latest progress in HEB technology was made with HEBs based on ultrathin NbN films. With 3-4nm films a mixer gain bandwidth of 3-4GHz has been achieved. It corresponds to 5-6GHz receiver noise bandwidth (doubling the receiver noise temperature) [4]. The receiver noise temperature as low as 450 K at 600 GHz [4], 490 K at 840 GHz [5], 800 K at 1.1 THz [6], 700 K at 1.6 THz, 1100 K at 2.5 THz [7], 5600 K at 4.3 THz and 8800 K at 5.2 THz [8]. The present work was triggered by the development of 1.4-1.9THz NbN HEB mixers for the HIFI instrument of the Herschel Space Observatory. We investigate stability of HEB receivers with regards to the bolometer size, type of the local oscillator, and IF chain.

The Allan Variance

To obtain the Allan plot used to determine the Allan time, the output power of a HEB receiver was sampled. We call the data points p_n , n=1,…N, where N is 10^3-10^4. These values are grouped in M groups of K data points and averaged within the groups

$$X_i(K)=\frac{1}{K}\sum_{n=1}^{K}p_{(iK+n)} \qquad i=0,...M \qquad M=N/K-1$$

The Allan variance is then calculated using

$$\sigma_A^2(K)=\frac{1}{2M}\sum_{i=1}^{M}\left(X_{i+1}(K)-X_i(K)\right)^2$$

The variance is plotted as a function of the integration time $\tau = Kt$, where t is the time between the data points [3].

There are three main contributions to be aware of in the Allan plot [4]. The first is the white noise. It follows the radiometer equation and has a slope equal to -1. It is the left part in the Allan plot, see fig. 1. The second contribution is the 1/f-noise which has a slope equal to zero and will therefore not be reduced by longer integration. The last contribution is low frequency drift noise. This has slope ≥1 and is usually found for longer integration time in the Allan plot. Thus longer integration time will only give less efficient observations and not lower noise level if drift noise is present. These three contributions can be summarized as

$$\sigma_A^2(T)=\frac{a}{T}+b+cT^{\alpha}$$

Where a, b and c are appropriate constants. The Allan time (T_A) is defined as the integration time where the Allan plot deviates from the radiometer equation. Integration longer than the Allan time is not efficient and might reduce signal to noise ration.

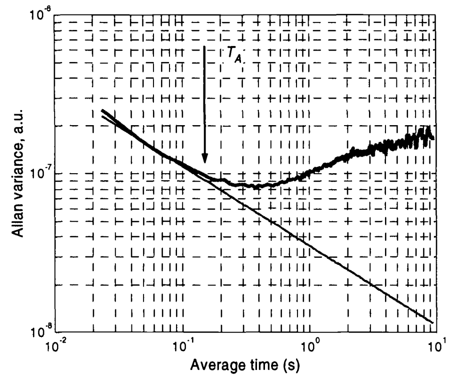

Figure 1 A Allan variance plot. The straight line shows the radiometer equation. The leftmost slope shows how white noise is integrated down, the middle (horizontal) part is dominated by the 1/f-noise and the right slope comes from a slow drift.

NbN mixers and set-up.

HEB mixers with bolometer size of 4x0.4 μm^2, 3x0.2 $\mu m^{2,}$ 2x0.1 μm^2 and 1x0.15 μm^2 were used in the investigation. The mixers are made of 3.5 nm thick NbN films. The films are processed with e-beam lithography as described in [9]. Bolometers were integrated with gold planar double slot antennas (DSA). The FTS response of the DSA antenna integrated HEBs peaked at 1.6THz [13].

Three types of local oscillators were used: a FIR gas laser, a solid state source and a Backwards Wave Oscillator (BWO). The former is a ring gas laser pumped with a CO_2 laser. CH_2F_2 gas provided 1.63 THz, 1.89 THz and 0.69 THz lines. The output power is on the level of 1-4mW. The solid state source is a chain consisting of three power amplifiers and four doublers. The chain is pumped with a 95 GHz Gunn diode oscillator to obtain an output signal of 1-2 μW at 1.5 THz [10]. As an alternative to the Gunn oscillator, a 15.8GHz synthesizer with x6 multiplier was also used with the same THz output power. The solid state source is a Band 6 Low LO prototype for the Herschel Space Observatory [11]. The BWO radiates at approximately 600 GHz with output power at mW level. The laser was free running without feedback loop control. The Gunn oscillator was verified both with feed back loop and without. No difference on the receiver stability has been observed for both cases. In order to verify the spectral purity of the FIR laser and the solid state source, we performed a mixing of both at about 1.5THz with the laser as LO.

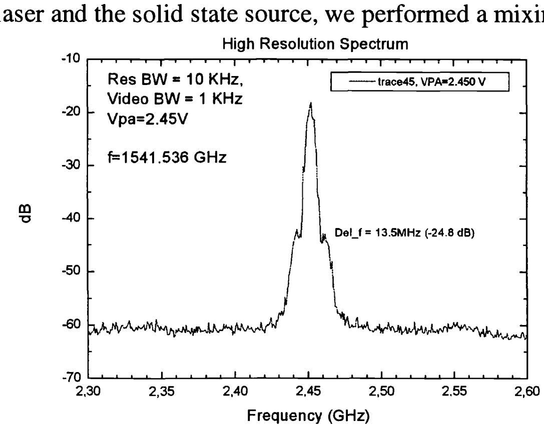

Figure 2. Mixing signal of the solid state source and the FIR laser as LO.

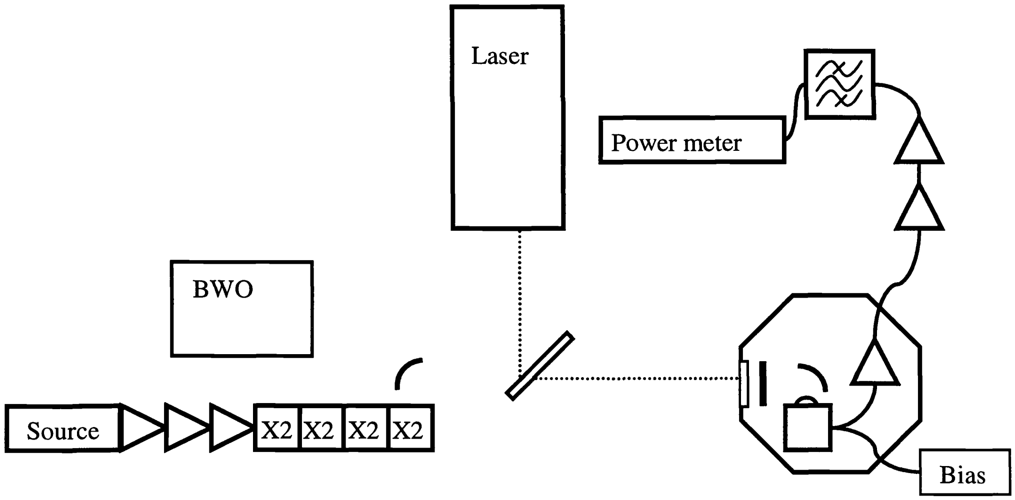

Figure 3 The setup layout: LO sources, beam splitter (only used with the laser); cryostat with the mixer unit, off-axis paraboloid and an LNA; room temperature IF chain with two Miteq amplifiers, a 30 MHz YIG filter and the power meter.

To measure the noise temperature of the receiver, the Y factor method is used. The cold load is an absorber in a bath of liquid nitrogen placed approximately 50 cm from the mixer. The radiation is transmitted via a mirror and chopped with the hot load, i.e. a chopper covered with Eccosorb at 295 K. During measurements with the FIR laser the LO signal is coupled into the mixer via a beam splitter made of thin polyethylene. An elliptical mirror and a parabolic mirror were used to match the beams of the LO and the mixer. Verification of the noise temperature of the HEB receiver were done with the FIR laser, as well as with the BWO. The noise temperature results are not corrected for the input optical loss (unless indicated additionally).
The HEB chip is glued on a 5 mm elliptical lens mounted in a HIFI band 6 prototype mixer unit. It is connected to a 2-4 GHz InP LNA [12] without an isolator in between. The bath temperature is 4.2K.
The signal from the mixer is further amplified at room temperature with two 0.1-12 GHz Miteq amplifiers and filtered with a YIG-filter. The bandwidth of the filter is 30 MHz and it is tuned close to 2 GHz. A HP power meter E4419B with an E4412A power head is used as IF detector. The detected signal is sampled with 1/(24 msec) rate with the help of GPIB and Labview.

Experimental results

1.6THz FIR laser.
We start description of the experimental results with measurements at 1.63THz with the FIR laser as an LO source.
HEB mixers are patterned in a shape of a superconducting bridge. Therefore, at no LO power there is no power dissipation in the HEB until bias current exceeds the critical current I_c and the bridge switches into resistive state. Two regions in the resistive state are distinguished: stable and unstable. Unstable resistive state is created when the bias current just exceeds the critical current. The dissipated power (both LO and dc, or dc only if LO is off) is not enough to maintain the hot spot (resistive domain in the superconducting bridge). The bridge switches between superconducting state and resistive state. As the dissipated power grows, the hot spot becomes stable. It happens either at higher bias voltages or (and) large LO power. Applied LO power suppresses superconductivity, i.e. decreasing I_c. Finally, at very large LO power the bridge remains in the resistive (normal) state even when the bias current (voltage) is zero. The highest sensitivity for the NbN HEB mixers is obtained when there is only the superconducting state and the stable resistive state on the IV curve. A set of such IV curves is shown in Figure 4. Two

upper IV curves still contain unstable region at small bias voltages. Therefore, they are stopped at the lowest bias when the mixer is still stable.

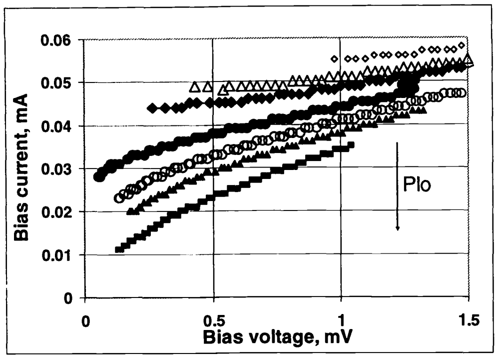

Figure 4. A set of IV curves for different LO power levels.

There is an optimal LO power corresponding to the lowest HEB mixer noise temperature. Dependence of the mixer noise temperature vs bias current at 0.5mV bias voltage is shown in Figure 5. The IV curve recorded under the optimal LO power is called the optimal IV. For such IV curve the mixer noise temperature is a function of bias voltage with a wide minimum. The position of this minimum depends on the bridge size. Figures 4 through 6 are given for $2x0.1\mu m^2$ bridge size. We investigated stability of HEB receivers both at the optimal point (with the lowest noise temperature) as well as at the other bias points.

For example, driving the mixer to the normal state (very large LO power or (and) high bias voltage) allows us to investigate stability of the IF chain noise. Indeed, in the normal state the HEB mixer is just a resistor at an effective temperature equal to the critical temperature of the superconductor (9-10K in our case). However, we can not draw any conclusions about IF gain stability this way. A signal much bigger than the IF noise has to be applied instead of the mixer. However, verification of the IF stability with the mixer in the normal state is a good test for the IF part of the receiver.

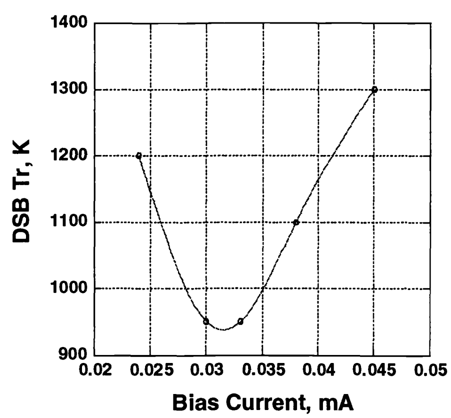

Figure 5. Tr(corrected) vs bias current (also vs LO power) at the optimal bias voltage (0.5mV).

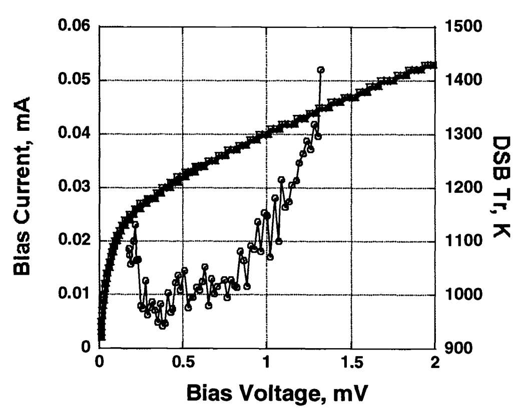

Figure 6. Optimal IV curve and the corresponding Tr(corrected) vs bias voltage dependence.

We start with the $4x0.4\mu m^2$ mixer which was driven into the optimal operation point (1.2mV, 60μA) at 1.63THz laser frequency. The IF frequency was 2GHz , i.e. at the lower end of our 2-4GHz low noise amplifier (LNA).

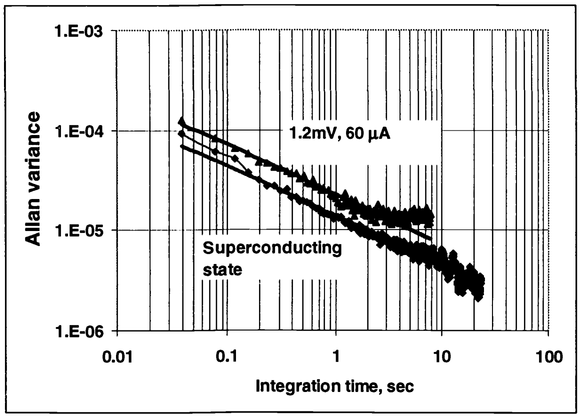

Figure 7. Allan variance for 4x0.4μm^2 HEB mixer (with 1.6THz DSA) with 1.63 THz FIR laser as LO. 2GHz IF; optimal bias and LO power.

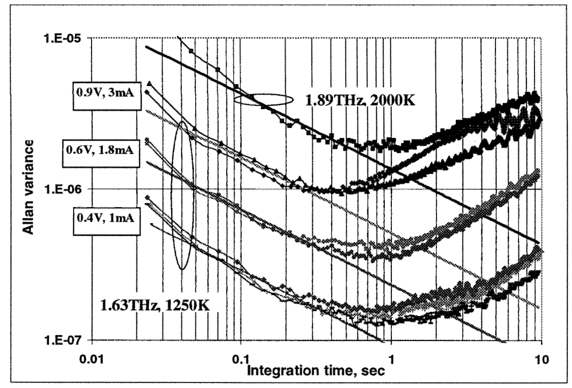

Figure 8. Allan variance for 3x0.2μm^2 HEB mixer (with 1.6THz DSA) with 1.63 THz and 1.89 THz FIR laser as LO. Measured (uncorrected) receiver noise temperatures are also indicated. 2GHz IF; optimal bias and LO power. At 1.6THz the curves are grouped for different LNA bias.

The Allan variance follows the radiometer equation up to 3sec after which the 1/f noise becomes visible and the curve becomes horizontal (see Figure 7). Switching the mixer into superconducting state (no LO power and zero bias current) is equivalent to the situation when the mixer is in the normal state. The difference is only the input impedance for the LNA. Still with zero Ohm input load the IF chain noise had stability better that 10 sec.

As the mixer size decreases to 3x0.2μm^2 the Allan time decreases to 0.4 sec. In Figure 8 the Allan plots are presented for such mixer integrated with the 1.6THz double slot antenna (DSA) at both 1.63THz and 1.89THz LO frequency with the FIR laser as LO. At 1.89THz the receiver noise temperature is almost twice as much as at 1.63THz. However, the Allan time is 0.4 sec, i.e. the same as at 1.63 THz. In Figure 8 one can observe a slight influence of the LNA bias on the overall receiver stability. With the LNA drain bias of 0.9V and 3mA the Allan time of the receiver reduces to 0.3sec. Receiver noise temperature was found to be the same from 0.4V to 0.9V of the HEMT's drain voltage.

Results for the mixers of 2x0.1μm^2 and 1x0.15μm^2 size are presented in Figure 9 and Figure 10. These mixers have nearly the same volume and the resulting Allan time is also very close, i.e. 0.1-0.2 sec. The results for 2x0.1μm^2 device are given for different bias currents (i.e. different LO power) at the optimal bias voltage. The optimal current was 33 µA. As the LO power increases the receiver becomes more stable, however it is accompanied by the growth of the receiver noise temperature. As the mixer approaches the normal state (lowest curve) the receiver stability becomes defined by the IF chain and the Allan time extends up to a few seconds (limited by the measurements accuracy). The results for a 1x0.15μm^2 device are compared for different bias voltages while the LO power was kept at the constant (optimal) level. The tendency is the same as for the previous sample, with the Allan time of 0.1-0.2 sec at the optimal biasing and up to 10 sec at the high bias voltage, when the mixer becomes normal. For both LO power and bias voltage variation, a noticeable increase of the receiver stability is achieved only for the regimes when the receiver noise temperature is significally higher than its value at the optimal point.

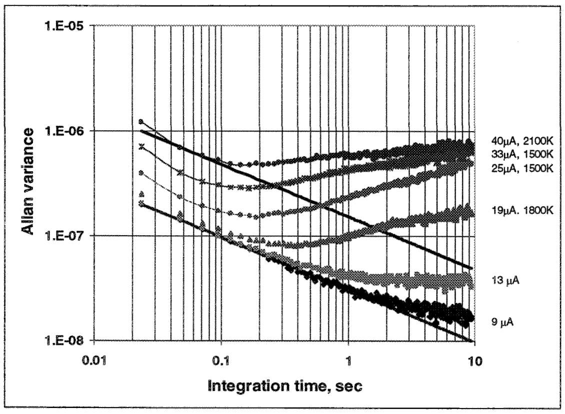

Figure 9. Allan variance for 2x0.1μm^2 HEB mixer (with 1.6THz DSA) with 1.63 THz FIR laser as LO. 2.5 GHz IF.

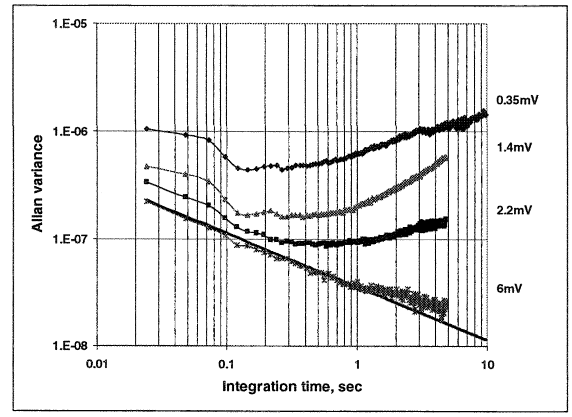

Figure 10. Allan variance for 1x0.15μm^2 HEB mixer (with 1.6THz DSA) with 1.63 THz FIR laser as LO. 2GHz IF.

Solid state LO at 1.5 THz.

As we will discuss in the next chapter, a strong influence on the receiver stability comes from the LO source. For example, the power stability from the FIR laser is influenced by the mechanical stability of the mirrors in the FIR resonating cavity. Therefore, a different type of the LO source was involved in the experiment: a solid state source at about 95GHz followed by power amplifiers and doublers. The output THz power of the multiplier chain is much smaller than from the laser. Therefore the coupling optics was carefully designed in order to provide sufficient LO power to drive the HEB mixer. For this reason, only small mixers were tested, which LO power requirements fit to the available power. The mixer noise temperature was measured in advance with the FIR laser (which high power allowed us to use a thin beam splitter). From this test we obtained the optimal IV curve (optimal LO power) and the optimal bias voltage.

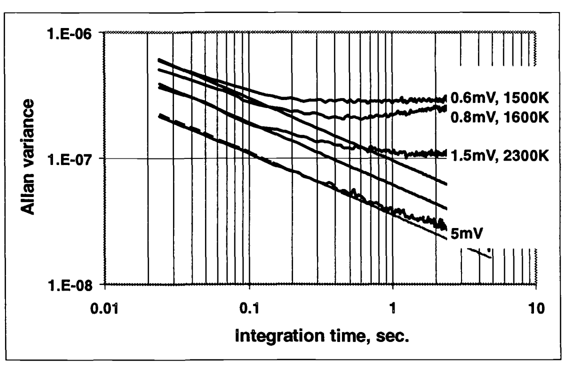

Figure 11. Allan variance for 1x0.15μm^2 HEB mixer (with 1.6THz DSA) at 1.5 THz with the solid state LO. IF is 2.5 GHz.

With the solid state source the mixer was pumped to the optimal IV curve and the Allan variance was measured at a variety of the bias voltages (see Figure 11). At 0.6V, where the mixer has the lowest noise temperature an Allan time of 0.15 sec was measured. At 0.6mV the Allan variance was also measured at three different LO power levels +1dB and -1dB off the optimal value, with the same obtained Allan time. During the experiment the LNA bias was varied in the range from 0.4V to 0.8V. We did not observe any influence of the LNA bias on the receiver stability.

Measurements at 0.69 THz and 0.6THz.

The 2x0.1 μm^2 device was also measured with a BWO at 0.6 THz and the FIR laser at 0.69 THz. The results are presented in Figure 12 and Figure 13. The measurements are done at the optimum bias point of the device. We found much stronger effect of the LNA bias on the receiver stability comparing to the results at 1.6-1.9 THz. An Allan time of 0.4 sec was obtained with the laser for 0.4V and 0.5V HEMT's drain voltage, while for 0.6V the Allan time reduced to 0.2 sec. With the BWO, an Allan time of 0.5-0.6 sec was measured for 0.4V and 0.5V of the drain voltage, and 0.3 sec for 0.6V. By maximizing the LNA gain (made by increasing the drain current to 3 mA) the Allan plot deviated from the radiometer equation from the very beginning, indicating an increased contribution of 1/f noise, which comes from the LNA.
The double slot antenna of this mixer is designed for 1.6 THz. Experimental investigation of the antenna coupled HEB response vs RF frequency we presented in [13]. At 0.6THz a Y-factor of 0.2-0.3 dB was measured. It means that the receiver was still able to detect instabilities in the RF path.

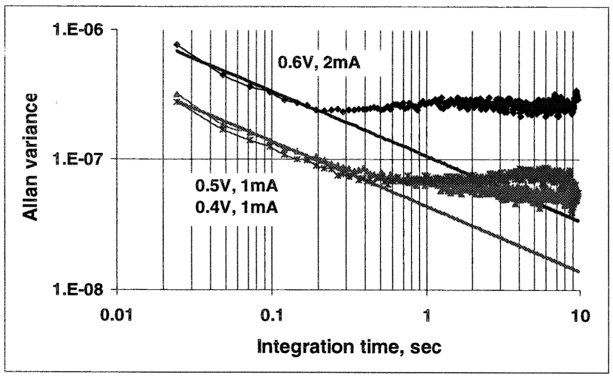

Figure 12. Allan variance at 0.69THz LO frequency (FIR laser). IF is 2.5GHz

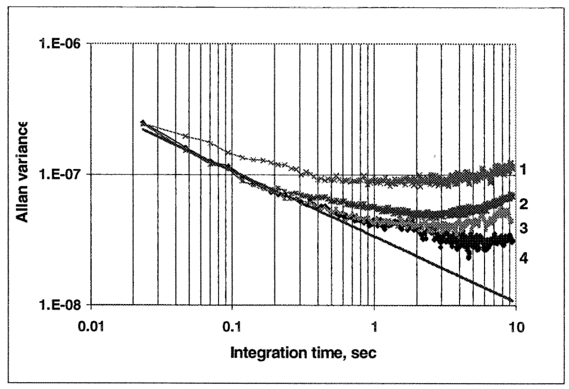

Figure 13. Allan variance at 0.6THz LO frequency (BWO). IF is 2.5GHz. LNA biasing: curve 1 0.6V,3mA; curve2 0.6V,2mA; curve3 0.5V,1mA; curve4 0.4V,1mA.

Discussion

During the Allan variance measurements it is the output receiver noise that is sampled. Therefore, in order to understand the obtained results we have to analyze the contribution from all parts of the receiver to the output noise. A signal chain of the HEB heterodyne receiver is shown in the diagram below.

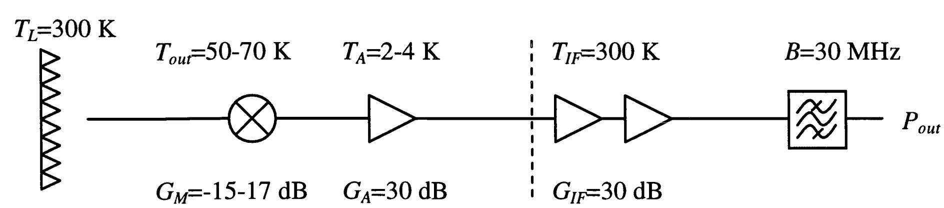

The total output power is

$$P_{out} \propto \left[2 \cdot T_L \cdot G_M(U_0, P_{LO}) + T_{out}(U_0, P_{LO}) + T_A\right] \cdot G_A(U_d) \cdot G_{IF}(U_{IF}) + T_{IF} \cdot G_{IF}(U_{IF}),$$

where T_L is the input load, G_M is the mixer gain which is a function of the mixer bias and LO power, T_{out} is mixer output noise which also depends on the mixer bias and the LO power. LNA input noise temperature T_A we assume to be constant, while the amplifier gain G_A depends on the HEMT's drain voltage U_d. Room temperature amplifiers contribute with the "constant" noise temperature T_{IF} and bias dependent gain. With the noise budget shown in the diagram, when the mixer is in the operation point its noise dominates over the LNA noise by 5÷10dB. Therefore mixer bias and LO power fluctuations will be visible at the output. Down converted signal from the input load is visible by 0.3-0.8dB (Y factor) above the mixer noise. The load signal is influenced by the mixer gain, and therefore by the mixer bias and the LO power. Both the LNA's gain G_A and the room temperature amplifier gain G_{IF} directly affect the output noise stability. For an ideal receiver, when bias voltage and LO power are infinitely stable, the spectrum of the output noise shall be white, perhaps affected by 1/f noise only sourcing from the amplifier's gain. In the HEB the main contributor to its noise is the thermal fluctuation noise caused by the .heat exchange between electrons and the heat bath (phonons of the superconducting film and of the substrate). Since the time constant of this heat exchange is of the order of 40 psec its spectrum shall be white. Extra spectral components in the mixer noise can be produced by instabilities of the mixer bias and of the LO power. Considering the mixer bias, both a voltage source with a feed back loop of more than 1kHz and a free running source (output impedance of about 1kOhm) were used in the present experiment. We did not observe any influence from the type of the biasing on the receiver stability. In the case of the free running source (which is indeed very close to a current source), the load line of the mixer bias point is nearly horizontal (when the LO power changes the change of the mixer voltage is much bigger than the change of the mixer current). At the optimal bias point the dP/dU is quite small (see Figure 14; the optimal point is marked with a circle). Simultaneously, dP/dI is much bigger. We can conclude that in case of the voltage source the LO power stability is crucial (dP/dI), while for a current source the effect of LO power fluctuations is expected to be reduced.

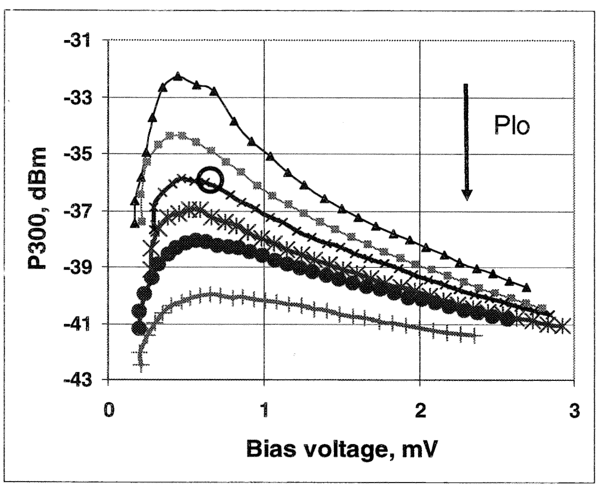

Figure 14. Receiver output noise (with 300K load) as a function of mixer bias.

With a FIR laser a source of power instabilities are mechanical vibrations and drifts in the resonator mirrors. It has been observed that at certain regimes the laser emission line gets a strong phase noise. It results in a jump of the receiver output noise as well as the receiver noise temperature.

In case of the solid state source, power fluctuations might be caused by the driving power instabilities and by the contribution from the power amplifiers and the multipliers. We verified the receiver stabilities with both Gunn oscillator and a synthesizer. Different power amplifier bias points have been used as well. None of the mentioned steps had an influence on the Allan time of the receiver. A possible source of the receiver instabilities can be originating from the atmosphere transmission oscillations.

This aspect is analyzed in [14] and will not be discussed in this paper. A strong support for this source is given by the fact that the Allan time reduces as the HEB mixer size decreases, reducing the optimal LO power and making the mixer more sensitive to LO power variations. Additionally, results at 0.69 THz and 0.6THz indicate and increase of the Allan time to 0.4-0.5 sec for small HEBs.

Simultaneously, at 0.6-0.69Thz for small HEBs and at 1.6-1.9THz for bigger (3x0.2 μm^2) HEBs the receiver stability becomes dependent on the LNA bias, which is not visible for small HEB at 1.6THz for example. This influence comes with 1/f noise from the LNA gain.

Conclusions

We investigated the stability of the NbN HEB heterodyne receiver at frequencies from 0.6THz to 1.9THz with three different LO sources: a FIR laser, a x16 multiplier chain and a BWO. We found that for 4x0.4 μm^2 bolometer size anAllan time as large as 3 sec can be obtained at THz frequencies with 30MHz instantaneous bandwidth. As the mixer becomes smaller the Allan time reduces to 0.5sec for 3x0.2 μm^2 mixers and 0.1-0.2sec for 2x0.1 μm^2 and 1x0.15 μm^2 mixers. With the 1x0.15 μm^2 mixer the receiver stability was the same with both FIR laser and the multiplier chain. At 0.6THz and 0.69THz the Allan time of 0.5sec can be obtained with both BWO and the FIR laser as the LO source.

Acknowledgements:

The authors are grateful to: the Moscow State Pedagogical University (Moscow, Russia) for deposition of thin NbN films; Jet Propulsion Laboratory (Pasadena, USA) for making the x16 multiplier chain available for the experiment; and to the Space Research Organization of the Netherlands for the help with x16 chain test.

References:

1 Optimization of heterodyne observations using Allan variance measurements. R.Schieder, C. Kramer. Astronomy and Astrophysics, v. 373, p. 746-756, 2001.

2 Noise stability of SIS receivers. J.W. Kooi; G. Chattopadhyay; M. Thielman; T.G. Phillips; R. Schieder. International Journal of Infrared and Millimeter Waves, v 21, n 5, May, 2000, p 689-716.

3 E. M. Gershenzon, G. N. Gol'tsman, I. G. Gogidze, A. I. Elant'ev, B. S. Karasik and A. D. Semenov, "Millimeter and submillimeter range mixer based on electronic heating of superconducting films in the resistive state", Sov. Phys. Superconductivity, 3, 1582, 1990.

4 S. Cherednichenko, M. Kroug, P. Khosropanah, A. Adam, H. Merkel, E. Kollberg, D.Loudkov, B. Voronov, G. Gol'tsman, H.-W. Huebers, H. Richter, "1.6 THz HEB mixer for far infrared space telescope (Hershel)", Physica C, vol.372.pp.427-431, Aug. 2002.

5 Tong C-Y, et al, *Proc. 11th Int. Symp. on Space Terahertz Technology*, Ann Arbor, MI, 49, 2000.

6 S.Cherednichenko, M. Kroug , P. Khosropanah, A. Adam, H. Merkel, E. Kollberg, D. Loudkov, B. Voronov, G. Gol'tsman, H. Richter, H.-W. Hübers, "A BROADBAND TERAHERTZ HETERODYNE RECEIVER WITH AN NbN HEB MIXER", *Proc. 13th Int. Symp. on Space Terahertz Technology*, Cambrige, MA, 2002.

7 M.Kroug, S.Cherednichenko, H.Merkel, E.Kollberg, B.Voronov, G.Gol'tsman H.-W.Huebers, H.Richter' "NbN HEB mixer for terahertz heterodyne receivers", IEEE Trans. on Appl. Supercond. Vol.11, n.11, pp. 962-965, 2001

8 A.D. Semenov, H.W. Huebers, J. Schubert, G. Gol'tsman, A.I. Elantiev, B. Voronov, and G. Gershenzon, "Design and performance of the lattice cooled hot-electron terahertz mixer", J.Appl.Phys. **88** (11), p.6758, 2000.

9 M. Kroug, P. Yagoubov, G. Gol'tsman and E. Kollberg, "NbN quasioptical phonon cooled hot electron bolometric mixers at THz frequencies", *Proc. the 3rd. European Conference on Applied Superconductivity*, Veldhoven, Netherlands, (Inst. Phys. Conf. Ser. No 158, p.405), 1997.

10 Measured with Thomas Keating THz power meter prior the experiment.

11 A.Maestrini et al., ", *Proc. 13th Int. Symp. on Space Terahertz Technology*, Cambrige, MA, 167, 2002.

12. N. Wadefalk, A. Mellberg, I. Angelov, M.E. Barsky, S. Bui, E. Choumas, R.W. Grundbacher, E.L. Kollberg, R. Lai, N. Rorsman, P. Starski, J. Stenarson, D.C. Streit, H. Zirath, "Cryogenic wide-band ultra-low-noise IF amplifiers operating at ultra-low DC power", IEEE Trans. on Microwave Theory and Techniques, vol. 51, No. 6, pp. 1705-1711, June 2003.

13 D. Loudkov, P. Khosropanah, S. Cherednichenko, A. Adam, H. Merkel, E. Kollberg, G. Gol'tsman, "Broadband Fourier Transform Spectrometer (FTS) measurements of spiral and double- slot planar antennas at THz frequencies", *Proc. 13th.* International Symposium on Space Terahertz Technology, *Cambridge, MA , March 2002.*
14 "Regarding Atmospheric and Mechanical Stability Requirements of (LO-pumped) Mixers", J.W. Kooi, R. Schieder. Proc. Fifteenth International Symposium of Space Terahertz Technology, 2004